



Article citation info:

Sawczuk W, Merkisz-Guranowska A, Rilo Cañas A-M. Assessment of disc brake vibration in rail vehicle operation on the basis of brake stand. *Eksploracja i Niezawodność – Maintenance and Reliability* 2021; 23 (2): 221–230, <http://doi.org/10.17531/ein.2021.2.2>.

Assessment of disc brake vibration in rail vehicle operation on the basis of brake stand

Wojciech Sawczuk^a, Agnieszka Merkisz-Guranowska^a, Armando-Miguel Rilo Cañas^b

^aPoznan University of Technology, Institute of Transport, ul. Piotrowo 3, 60-965 Poznan, Poland

^bDB Systemtechnik GmbH, Adlergestell 143, 12439 Berlin, Germany

Indexed by:



Highlights

- In the operation of a disc brake, the geometry of the system changes with the wear of the pads.
- The lever system is characterized by an uneven distribution of masses on the right and left side of the disc.
- There is a difference in the vibroacoustic signals of the right and left brake pads.
- The heavier side of the system shows greater friction in the joints and a reduction in pad vibration.
- The non-uniform vibrations of the friction pads indicate a disturbance in the braking process.

Abstract

The scientific aim of the article is to present the relationship between the vibroacoustic signals of the right and left friction pad during braking, depending on the mass distribution, as an element of the lever system. This article presents the results of tests of a railway disc brake in the scope of vibrations generated by pads in various states of wear located on both sides of the brake disc. The tests were carried out on the brake stand using the vibroacoustic method including the analysis of amplitudes and frequencies and the thermal imaging method. Special attention was paid to the analysis of the classic lever mechanism as a multi-mass system influencing the thermo-mechanical characteristics and vibrations of the pads on the right and left side of the brake disc. Uneven mass distribution of the system translates into uneven wear of the friction components. The scientific aim of this paper is to present the relation between vibroacoustic signals of the right and left friction pad during braking depending on the mass distribution of the lever system component.

Keywords

This is an open access article under the CC BY license (<https://creativecommons.org/licenses/by/4.0/>)

railway disc brake, brake vibration, lever mechanism.

1. Introduction

When scrutinizing the available literature sources, one may observe that the vibroacoustic processes generated by brake systems are analyzed in three directions. In the first, most numerous part, are works treating on the noise accompanying the braking process. In this respect, some of the researchers attempt to explore and identify the reasons for the occurring noise [8, 14, 15, 28, 41, 43]. Other researchers attempt to model the noise depending on the geometry features of the brake system and the components of the friction pair. The second, less numerous group of papers treating on the vibroacoustic processes in brake systems, constitute works on application of brake system vibrations in diagnostics of the wear level of a friction pair [29, 30]. The least numerous group of papers treating on vibroacoustics are works describing the use of brake system vibrations to evaluate the braking process itself. Simple analyses in the domain of amplitudes and frequencies to build regressive diagnostic models was applied in [28] that, upon transformation, allow assessing the value of the average coefficient of friction for selected braking speeds. Majority of models describing the vibrations of a brake system is based on the assumption that the increment of vibrations (a phenomenon heavily depending on a multitude of variables) is most dependent on the variability of the coefficient of friction between the brake pad and the brake disc. Additionally, the sensitivity of the brake system components (brake pads in

particular) increases or reduces the vibrations generated by the brake system and its emission to the environment, which is described in [19] as a strongly unfavorable phenomenon, and to a decrease in vibrations generated by the braking system, which is a favorable phenomenon. The collected results from the operation of the braking system enable the analysis of its reliability as described in [1, 9, 16, 32], and, consequently, the development of algorithms for estimation of the time to failure as presented in [31].

The vibroacoustic processes generated by friction in brakes refer to simple models in the literature. These are two-mass systems with only the friction pad and the disc considered. However, there is no description of the vibroacoustic phenomena generated by friction materials in complex braking systems in automotive or railway vehicles. In such cases, apart from the model of contact between the friction pad and the brake disc itself, the lever system of force transmission from the brake cylinder to the friction pads should also be taken into account.

2. Vibration models and a model of the disc brake lever system

The initial models assumed that self-induced vibration of a brake was related to the drop in the coefficient of friction and increased slip velocity [14, 22, 24]. These were models of the elastic friction system called the stick-slip phenomenon. On this basis, it was observed that

E-mail addresses: W. Sawczuk - wojciech.sawczuk@put.poznan.pl, A. Merkisz-Guranowska - agnieszka.merkisz-guranowska@put.poznan.pl
A-M. Rilo Cañas - Armando-Miguel.Rilo-Canas@deutschebahn.com

the necessary condition for vibroacoustic phenomena to take place in a brake is the dependence of the coefficient of kinetic friction on the increase in the velocity $\mu_o(v_2)$ assuming inequality (1):

$$\frac{d\mu_o}{dv_2} < 0 \quad (1)$$

where: μ_o – coefficient of kinetic friction,
 v_2 – velocity.

According to [14], if $\mu_2 > c/mg$, a self-induced vibration takes place generating the vibroacoustic phenomena, which, in the case of friction brakes, results in their squealing. It should be emphasized that the model of the stick-slip phenomenon of vibrations in the brake is correct in the case of a 1Bg single-block block brake. However, it does not work for the 2Bg double-unit block brake and disc brake.

Fosberry and Holubecki in [7] published theses that vibration in brake systems is caused by the cooperation of the brake pad-brake disc friction pair of the coefficient of static friction μ_{st} greater than the coefficient of kinetic friction μ_o or when the coefficient of kinetic friction increase with the increase in velocity v_2 . Similar conclusions were stated by Sinclair [34] and by Earles [4]. Other researchers such as Mills, Bowden and Leben [2] conducted research on resilient friction systems comparing them to the stick-slip motion [43, 44]. Eventually, the researchers declared that the vibroacoustic phenomena were not fully explored but their most likely explanation is the stick-slip motion in the friction coupling, whose source of energy is the change in the coefficient of friction as a function of velocity.

Spurr, in [37] proposes a term 'sprag-slip' to describe vibroacoustic phenomena in brake systems. He claims that the vibroacoustic phenomena generated by brake systems result from the contact of the friction pad with the brake disc. The friction force in such a system may be much greater than the same force in an ideally rigid system. In an actual brake system, due to elastic deformations and displacements, cyclic instantaneous drop and increase in friction occurs. This particular case was described by Spurr as spragging. Later, this model was improved by Jarvis and Earles [4, 14].

This was the first attempt of a theoretical explanation of the sprag-slip phenomenon, in which, in order to explain vibroacoustic phenomena, a rotating plate with a support was used. Later models, based on the Jarvis, Mills and Earles considerations, were more complex, had more degrees of freedom and several models of friction [21]. It should be emphasized that in the case of the sprag-slip phenomenon, despite the unilateral impact of the brake block (slider) on the brake disc, the researchers introduced a variable in the form of the slider inclination angle. It is a model of vibroacoustic phenomena the most similar to the real braking system. The angle of inclination of the slider corresponding to a change in the setting of the friction pads in relation to the brake disc has been taken into account in the model [36].

As Crolla and Lang [3, 17], have proven, this and other models do not entirely reproduce the actual brake. Yet, thanks to these models, one may obtain a qualitative indication for the process of design and search for solutions eliminating some classes of brake vibration, hence, the generated noise.

Then, Lang and Smales in [17] distinguished two types of vibroacoustic incidents originating in the brake systems. These distinctions are applied to date (phenomena occurring at low frequencies i.e. from 1 to 5 kHz and phenomena occurring at high frequencies, above 5 kHz.) The Lang's and Smales' model for low frequencies admits brake pads as rigid bodies. At high frequencies, one needs to additionally allow for deformations of the friction components. The assumption of a rigid body as a friction material was also utilized by Brooks [3], Milner [20] and Rudolph and Popp in their works [25, 26].

It should be emphasized that the models of vibroacoustic phenomena in brakes described in the literature concern a single disc and single pad system. In reality, a friction disc brake consists of a rotating disc

to which friction pads are pressed from both sides. The models available in the literature analyse only the case of the friction pad acting on one side of the disc, assuming that the same phenomena and relations will occur on the other side of the brake disc. In this paper, an attempt has been made to present vibrations generated by friction pads on two sides of a brake disc, which differ from each other in amplitude values, and to present an analysis of probable reasons for the difference in these vibrations. Additionally, results of friction-mechanical and thermovision tests with significant differences in temperature values of individual friction linings are presented.

Railway disc brake is composed of a brake disc fixed to the axle and a lever mechanism [33]. The lever mechanism is composed of two main levers (right and left) connected with a central lever in the middle. On one end of the main lever, brake pad holders with the brake pads are fitted as well as the cantilevers and on the other end of the main lever there is a brake piston rod. The lever mechanism is fixed to the bogie frame at three points i.e. through the central lever and two cantilevers. Figure 1a and 1b presents the lever mechanism of a railway disc brake in two planes (side and top), while Figure 2 shows the diagram of the lever mechanism as a multi-mass model in the x-y and z-x plane.

When analyzing Figure 1c, it is noteworthy that, as the wear of the brake pads increases, in order to keep the constant distance of the brake pad and the disc (approx. 1mm [35]) when the brake is not active, the angles of the right and left levers must vary in the range $\alpha_1 = 0-13^\circ$. This is an interval of the angle value for the maximum admissible brake pad wear to the level of 5 mm (thickness of a new brake pad is 35 mm). Changes in the angle α_1 directly influence the values of forces acting on the brake pad holders.

The operation of the lever system in the z-x plane was then assessed. A diagram of the lever mechanism as a multi-mass model in this plane is shown in Figure 2b.

In the z-x plane, aside from the changes of the value of angle α_2 (Fig. 3b and 3c) due to the wear of the brake pads, additionally the action of the friction force on the contact point of the brake pads and the brake disc generates an inertia force F_{IIV} , which makes part of the lever mechanism drop or lift depending on the direction of the disc rotation. As a consequence, on the vertical levers (cantilevers) clamping or separating forces are applied. If the lever mechanism is lifted when the friction force is directed upwards, the upper brake pads in

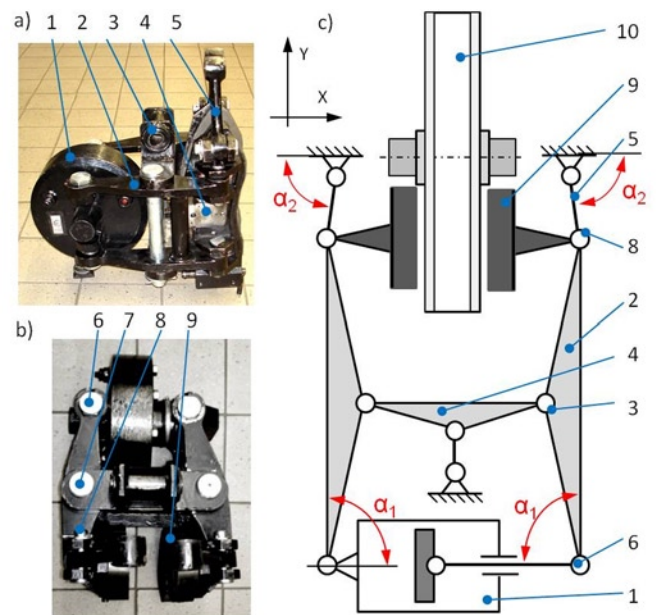


Fig. 1. View of the lever disc brake: a) side view, b) top view, 1-brake cylinder, 2-main lever (right and left), 3-central lever, 4-brake pad holder, vertical lever (cantilever), 6-brake cylinder pin, 7-central pin, 8-lever pin, 9-brake pad, 10-brake disc, c) structural model of the disc brake system

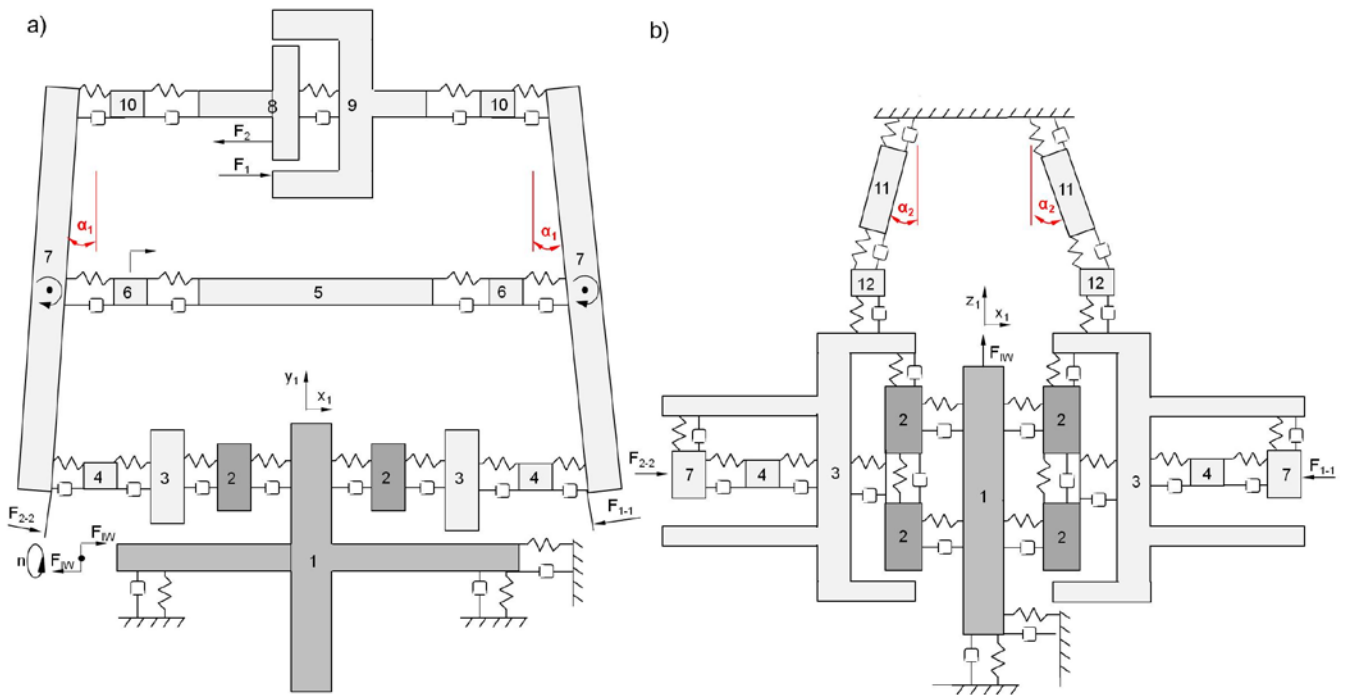


Fig. 2. View of the lever mechanism with visible parts as a multi-mass model in the plane: a) x - y b) z - x , 1- brake disc, 2- brake pad, 3- brake pad holder, 4, 6, 10, 12- pin, 5- central lever, 7- main lever (left, right), 8- piston rod, 9- cylinder, 11- cantilever, P_c - pressure in the cylinder, F_j - force from the piston rod, F_2 - force from the cylinder, $F_{1-1, 2-2}$ - forces acting on the brake pad holder with the brake pads, F_{w} - inertia force on the wheel circumference during braking, n - disc rotational speed, α_1 - angle of rotation of the main lever; α_2 - angle of rotation of the cantilever

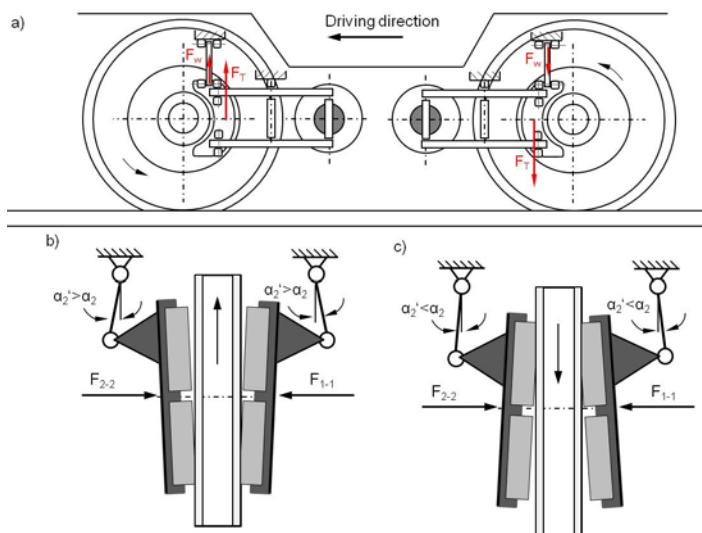


Fig. 3. Schematics of the bogie with a lever mechanism, a) forces acting on the lever mechanism during braking for a given driving direction, b) schematics of the brake pad setting when the friction force acts upwards, c) schematics of the brake pad setting when the friction force acts downwards, α_2' -angle of the vertical lever during braking, α_2 - angle of the vertical lever at the moment of stopping $v=0$

the holder separate from the disc which increases the inclination angle α_2 of the vertical levers. When the friction force is directed downwards, a separating force acts on the vertical levers and the lower brake pads in the holder are separated from the brake disc and the angle α_2 decreases. Figure 3 presents a diagram of the forces in the lever mechanism depending on the direction of rotation.

When analyzing the models presented in Figures 2a and 2b, one can observe that the railway disc brake, despite its simple design, is a multi-mass system [27]. Earlier research of the authors in the scope of identification of brake system vibration under laboratory (vibration frequency 4.5 kHz) and actual operation on a passenger railcar (vibration frequency 6 kHz) as well as those presented in [28, 30], confirm

that vibroacoustic phenomena occur at high frequencies. According to the Lang's and Smales's theory, friction components are masses susceptible to deformation. Other researchers such as Rudolph, Popp and North [23, 26] built a model of a disc brake caliper of a passenger vehicle of two degrees of freedom. Later, they expanded the model to six components, also of two degrees of freedom. They have observed that the vibroacoustic phenomena are influenced by the complexity of the brake system – the more components in the brake lever mechanism, the more components potentially generating vibroacoustic phenomena [26]. Besides, in [30] the authors draw attention to the fact that the main components of a brake system have a common resonance frequency, which also may contribute to the generation and amplification of vibroacoustic phenomena.

4. Analysis of the results of measurements of the masses of individual components of the disc brake lever mechanism

In order to assess the mass distribution of the complete brake caliper, all brake system components were dismantled and then weighed. Table 1 presents the masses of individual parts of the lever mechanism divided into left and right side of the clamping mechanism.

When analyzing Table 1, it can be observed that the sums of masses of individual components of the lever mechanism on the right and left side are not the same. The uneven distribution of the masses in the lever mechanism is influenced by the mass of the main levers (left and right) and the mass of the piston, in which the mass of the piston rod is almost twice as high as the cylinder. This is partly related to the additional mechanism of the piston rod, whose task is to set a constant clearance between the pads and the brake disc after braking (brake is disengaged) irrespective of the brake pad wear. Then, in the process of operation of the railway disc brake, as the brake pads wear, the angle α_1 increases on the main levers of the mechanism from 0 to 13° (in the case of the mechanism under analysis) and α_2 .

Table 1. Masses in kilograms of individual components of the clamping mechanism

No.	Component	Symbol	Mass on the left side	Mass on the right side	
1	Brake disc	m_1	116		
2	Brake pad	Upper	$m_{2,U,L}$, $m_{2,U,P}$	1.760	1.755
		Lower	$m_{2,D,L}$, $m_{2,D,P}$	1.745	1.750
3	Brake pad holder (caliper)	$m_{3,L}$, $m_{3,P}$	4.580	4.534	
4	Brake pad holder pin	Upper	$m_{4,U,L}$, $m_{4,U,P}$	0.858	1.452
		Lower	$m_{4,D,L}$, $m_{4,D,P}$	0.294	
5	Central lever	m_5	18.540		
6	Central lever pin	$m_{6,L}$, $m_{6,P}$	1.238	1.325	
7	Main lever	$m_{7,L}$, $m_{7,P}$	6.963	7.205	
8	Pneumatic brake piston	Piston rod	m_8	19.995	-
9		Cylinder	m_9	-	7.255
9'	Complete brake piston	m_8+m_9	27.25		
10	Pin of the brake piston	from cylinder (top and left)	$m_{10,U,L}$, $m_{10,D,L}$	0.259 i 0.258	-
		from the piston rod	$m_{10,P}$	-	0.275
11	Vertical lever (cantilever)	$m_{11,L}$, $m_{11,P}$	5.237	5.127	
12	Cantilever pin	$m_{12,L}$, $m_{12,P}$	0.370	0.372	
13	Washers, safety pins	m_x	0.182	0.088	
14	Sum of components on the left/right side	$m_{L,R}$	43.739	31.138	
15	Difference in left and right weight	r_w	12.60		
16	Complete lever mechanism	m_{2-13}	93.42		

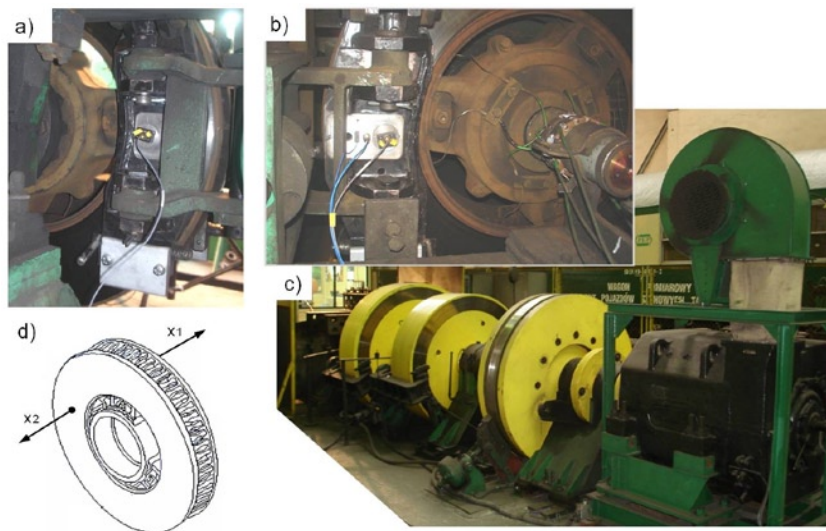


Fig. 4. Object of tests at the brake stand for testing railway disc brakes: a) view of the left brake support with a vibration transducer; b) view of the right brake support with a vibration transducer; c) view of the driving part of the brake position with rotating masses; d) orientation of vibration measurement directions

5. Methodology of tribological and vibroacoustic research

Friction-vibroacoustic research was conducted on the basis of the assumptions of the active experiment. During the tests, the input parameters, i.e. the state of the braking system, understood as wear of the friction pads, as well as such parameters as the braking start speed, pads pressure on the disc, mass to brake, were changed intentionally and in a specific way. Then, their impact on changes in output parameters was observed, such as the instantaneous and aver-

age friction coefficient, and acceleration of friction pad vibrations from the right and left of the brake disc.

The tests were carried out at a certified inertia brake stand, located at the Siec Badawcza Lukaszewicz - TABOR Rail Vehicles Institute in Poznan (Fig. 4). It is possible to perform tests on the rail block brake and disc brake reflecting the real conditions that occur when braking a rail vehicle. In addition, the Flir e60 thermal imaging camera was used during the tests to observe the temperature distribution of the friction linings after stopping braking.

The tests covered a ventilated brake disc with dimensions of $\text{Ø}610 \times 110$ made of gray cast iron. The brake disc has been prepared for tests in accordance with the standard [5, 6]. In accordance with the manufacturer's procedure and the requirements contained in the code [42], the pads were made of thermosetting resin, synthetic elastomer, metal and organic fiber as well as friction modifiers.

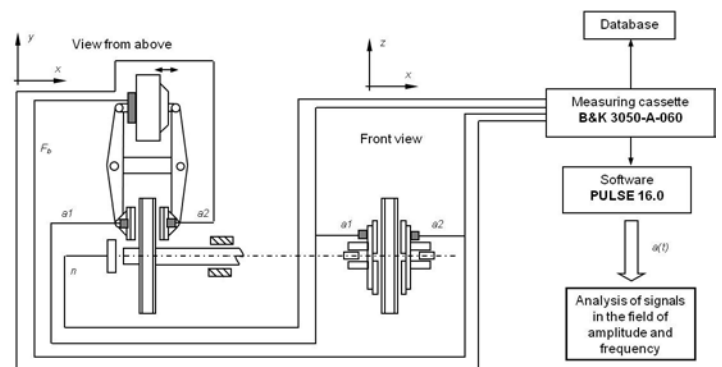


Fig. 5. Diagram of the measuring track used during vibroacoustic tests

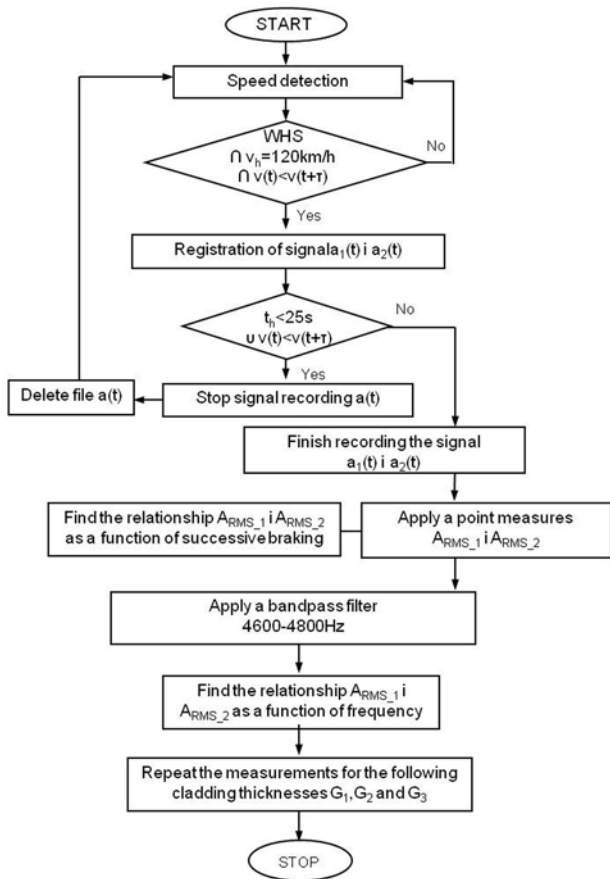


Fig. 6. Algorithm of vibroacoustic brake stand, *WHS* – perform stopping braking, τ – time gain

Three sets of pads were used for bench tests. The first new set of pads (4 pieces) with a thickness $G_1 = 35$ mm and two sets worn down to a thickness of $G_2 = 25$ mm and $G_3 = 15$ mm. Friction pad masses were $m_{G1} = 1.75$ kg (new pad), $m_{G2} = 1.45$ kg (pad worn up to 25 mm thick), $m_{G3} = 1.02$ kg (pad worn up to 15 mm thick), respectively.

Vibroacoustic tests were carried out in parallel with friction (tribological) tests. One vibration transducer (Fig. 4a and b) was attached to the brake mountings (right and left). The study was also carried out in accordance with the assumptions of the active experiment, where the input parameters were intentionally changed to record the output signals. The input values were simulated braking start speed v_0 , brake

pad pressure N , brake mass M , friction pad thickness G , and the output signals were instantaneous value vibration acceleration a . Then it was possible to observe the impact of input parameters on changes in output signals. B&K 4504A transducers were used to measure the vibrations. Figure 5 shows a diagram of the measuring track at the brake stand, additionally extended with the measurement of vibration acceleration.

When choosing the measurement site, the principle was adopted that the transducers should be located closest to the place generating the vibroacoustic signal associated with the operation of the brake friction pair and in a place easily accessible for measurement. The acceleration of vibrations was measured in a direction perpendicular to the surface of the brake disc, based on the experience of other researchers presented in [28, 38]. Figure 6 shows the algorithm of vibroacoustic brake stand.

6. Analysis of tribological test results

Friction tests carried out at a certified brake stand during braking in various combinations of brake lining pressure, braking masses, speed and degree of wear of the friction linings proved that in each braking case, wear is uneven on the piston rod and brake cylinder side. Also on the same side of the brake disc, the wear of the upper linings (above the rotational axis of the disc) as well as the lower ones varies. The set of weight consumption after 40 brakings for the lining pressure to the disc $N = 44$ kN, braking mass $M = 7.5$ t for five braking start speeds (50, 80, 120, 160 and 200 km/h) repeated 8 times, shown in Table 2. Wear tests of the friction material also included less lining pressure on the disc (28 kN) and less mass to be braked by one disc, i.e. 4.4 t. Similar studies on motor vehicles are described in [39].

In addition, during braking at the brake stand, there was a case of work of the stand as in the diagram shown in Figure 3c, i.e. the rotation of the brake disk pulls down the brake caliper. During the tests it was found that in each case of braking, both right and left bottom pads located in the brake mount wear slower. It was observed that in each case of braking, pads from the piston rod side (right side of the brake caliper) showed greater wear than pads from the brake cylinder side (left side of the caliper).

Due to the difficulty in determining the coefficient of slip friction, in the laboratory tests of the instantaneous coefficient of friction of the left and right side of the disc, the temperature distribution on the brake pads was determined with the thermo-visual methods. Figure 10 presents the temperature distribution on four brake pads after 40 instances of braking with the pressure $N=44$ kN and $M=7.5$ t.

Table 2. Consumption in grams of friction pads after 40 brakes with a pressure of $N = 44$ kN and a mass to brake $M = 7.5$ t

Weight consumption in grams of friction pads			
The pads New, thick $G_1=35$ mm		Pads worn to thickness $G_2=25$ mm	
Left side of the disc (from the brake piston rod)	Right side of the disc (from the brake cylinder)	Left side of the disc (from the brake piston rod)	Right side of the disc (from the brake cylinder)
Top pad	Top pad	Top pad	Top pad
117	129	115	123
Lower pad	Lower pad	Lower pad	Lower pad
112	114	105	112
Pads worn to thickness $G_3=15$ mm			
Left side of the disc (from the brake piston rod)	Right side of the disc (from the brake cylinder)		
Top pad	Top pad		
97	119		
Lower pad	Lower pad		
93	105		

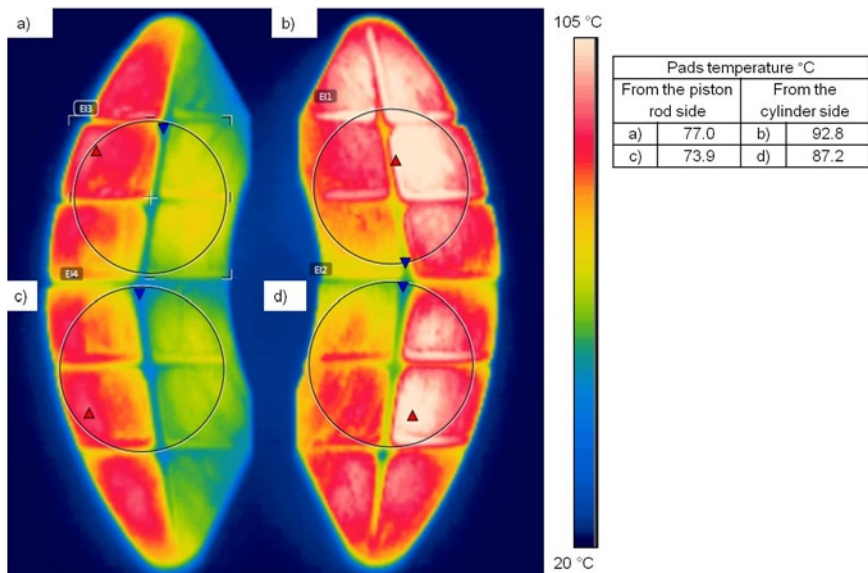


Fig. 7. Temperature distribution on the brake pads, a) upper left pad, b) upper right pad, c) lower left pad, d) lower right pad

When analyzing Figure 7, it is observed that the brake pads on the side of the piston rod have a higher temperature compared with the pads on the side of the cylinder. Besides, it can be observed that the lighter part of the brake cylinder i.e. piston rod, allows a better contact of the brake pads with the brake disc than the heavier brake cylinder. Higher temperature of the brake pads on the side of the piston rod translate into greater wear also on that side compared with the brake pads on the side of the cylinder. In addition, it was found that the difference in weight (12.6 kg) between the two brake cylinder assemblies also affects the frictional resistance in the bolt connections. It was observed that the right brake lever with the brake cylinder slidingly mounted on the central lever shows less resistance to movement in relation to the left brake lever with the piston rod.

7. Analysis of the result of vibroacoustic investigations

In the domain of amplitudes of analysis of vibration accelerations, point measures are most frequently applied that, with a single value, characterize a given vibration process in compliance with [29, 38]. Therefore, particularly in the vibroacoustic diagnostics (VD) it

is possible to determine changes in the VD signal resulting from the change of the technical state of an object. There is a variety of papers available in literature presenting the application of vibroacoustic diagnostics in vehicles such as passenger vehicles, railway vehicles or aircraft [11, 12, 13, 22, 40]. In order to determine the relation between the average coefficient of friction and the vibration generated by the brake system, in the first place the authors have confirmed that there is a relation between the vibration measured on the brake pad holders and the condition of the brake system understood as the brake pad wear. To this end, on the test stand, for all velocities under analysis, instantaneous vibration accelerations of the brake pad holders together with the brake pads were recorded. Figure 8 presents the relation of the instantaneous vibration accelerations as a function of the braking time for the brake pad holders together with the brake pads on the side of the piston rod and the brake cylinder.

Then, from the point measures, the RMS effective value of the vibration accelerations was determined according to [38] described with relation (2):

$$A_{RMS} = \sqrt{\frac{1}{T} \int_0^T [a(t)]^2 dt} \quad (2)$$

where: T – averaging time in [s],

$a(t)$ – instantaneous value of the vibration accelerations in $[m/s^2]$.

Then, applying the relation (2) from the instantaneous vibration accelerations for both pad holders, effective values were obtained for 40 instances of braking in the run-in process (speed 120 km/h). Figure 9 presents the ARMS relation for individual braking instances. From the experience gained during the test stand investigations of the disc brake, the authors know that the run-in of the pads is carried out for 25-30 braking instances after which (in conformity with [42]) over 75% of the surface is properly run in.

When analyzing the graph presented in Figure 9, one may observe that during subsequent braking instances performed under the same initial conditions (velocity, pressure, mass to be decelerated and disc

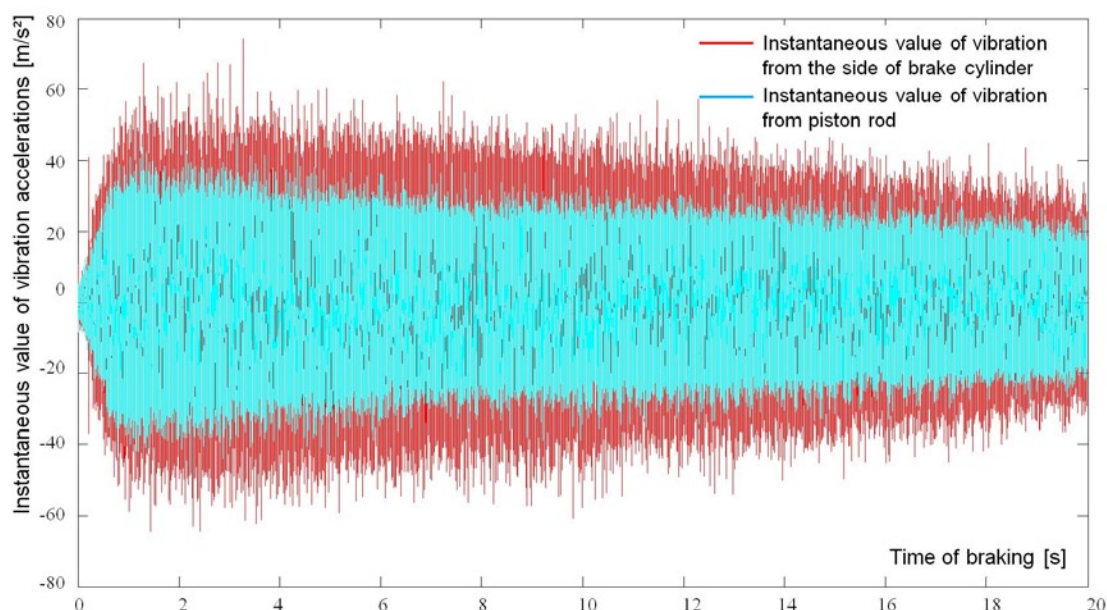


Fig. 8. Instantaneous value of the vibration accelerations of the brake pad holders during the first 20 seconds of braking from the speed of $v=120$ km/h, at the pressure of the pads on the disc $N=25$ kN and mass to be decelerated of $M=5.7$ tons

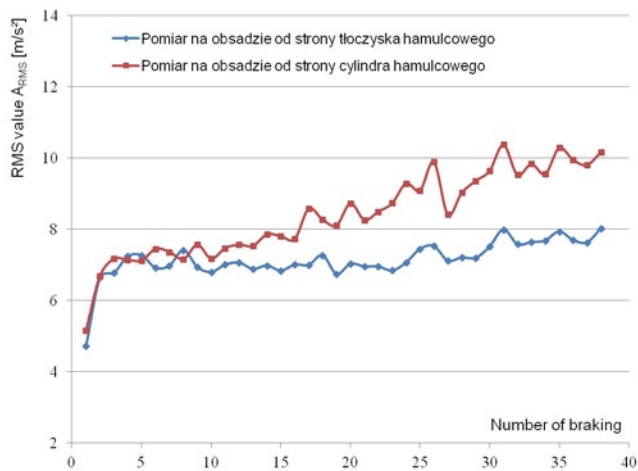


Fig. 9. Variability of the effective value ARMS of vibration accelerations for 40 braking instances during brake pad running-in

temperature), the difference in the vibration of the left and right pad holder increase reaching the highest value after the pads and the disc run in. However, on the side of the brake cylinder, the increment of vibration in subsequent braking instances is lower compared to the other side of the lever mechanism (the side of the piston rod). Besides, it was observed that, in the process of running in of the pads, the effective value of the accelerations increases, which is to be explained by the fact that in the first instances of braking not entire surface of the brake pads is pressed against the disc. When the pads are run in, after approx. 25 braking instances, the effective value of the vibration acceleration stabilizes on the level of approx. 10 m/s² for the pad holder on the side of the brake cylinder and approx. 8 m/s² for the holders together with the pads on the side of the piston rod.

When analyzing the graph presented in figure 9, it was observed that, according to relation 3 [28] as the brake pads run in with the brake discs, the dynamics of the changes of vibration between both sides of the brake discs increases. The dynamics of the changes increase from 1dB in the first braking instance to 3 dB after 30 braking instances at fully run in brake pads of the disc brake:

$$D = 20 \lg \left(\frac{A_2}{A_1} \right) \quad (3)$$

where: A1 – value of the point measure (ARMS) determined during braking on the brake pad holders on the side of the piston rod in [m/s²],

A2 – value of the point measure (ARMS) determined during braking on the brake pad holders on the side of the cylinder in [m/s²].

Next, an analysis of the signals of vibration accelerations in the frequency domain was performed. Figure 10 presents the spectrums of the vibration of the brake pad holders together with the brake pads (on both sides of the brake disc).

In the first place, for various braking (stopping and constant power), the frequency bands associated with the change in wear of the friction pads in the range of their thickness from 15 to 35 mm are determined, which directly influences the change in the geometry of the lever system. The α_1 (Fig. 1c) and α_2 (Fig. 3b and 3c) Angles change at the same time as the wear pads are worn in the lever mechanism. Frequency analysis has shown that in the 4600-4800 Hz frequency band is observed to change the effective vibration acceleration of friction pads both on the right side of the brake disc (brake cylinder side) and to the left of the disc, i.e. From the piston rod. For this frequency range, the dynamics of the change described by the dependence (3) in the vibrations of the pads new to the worn-out exceeds 6 dB. Table 3 shows the ARMS values for each of the vibration frequency bands of the friction pads of different thicknesses on the two sides of the brake disc during braking. Figure 11 graphically illustrates the dependence

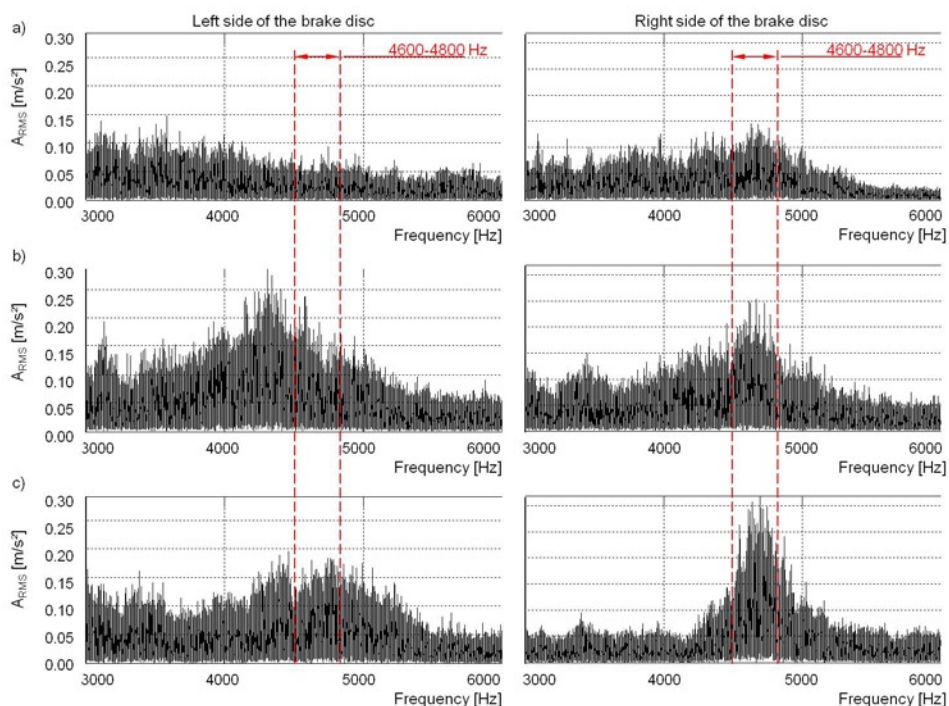


Fig. 10. ARMS dependence on frequency for two brake mounts with friction pads for the right and left sides of brake disc, a) for new pads, thicknesses $G_1=35$ mm, b) for pads worn to thickness $G_2=25$ mm, c) for pads worn to thickness $G_3=15$ mm

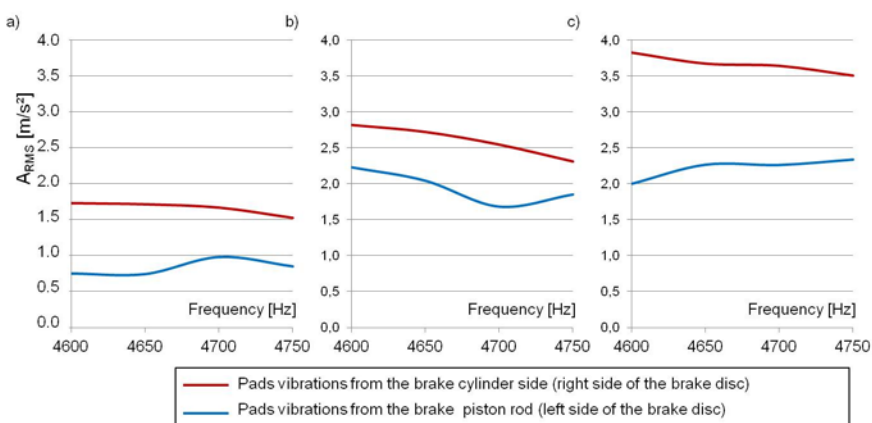


Fig. 11. ARMS relationship in the frequency band 4600-4750 Hz for two brake mounts with friction pads for the right and left of the brake disc, a) for new pads with a thickness of $G_1 = 35$ mm, b) for pads worn up to a thickness of $G_2 = 25$ mm, c) for pads worn up to a thickness of $G_3 = 15$ mm

Table 3. Statement of the ARMS values of the pads vibrations on the right and left side of the brake disc for 4600-4800 Hz band for three cases of friction material thickness during braking

For new pads thicknesses $G_1=35$ [mm]				
Frequency [Hz]	ARMS-2 pads on the left side of the disc [m/s^2]	ARMS-1 pads on the right side of the disc [m/s^2]	Vibration difference [m/s^2]	Dynamics of change [dB]
4600-4650	0.754	1.728	0.974	7.208
4650-4700	0.745	1.712	0.967	7.226
4700-4750	0.978	1.667	0.688	4.630
4750-4800	0.850	1.524	0.673	5.066
For pads worn to thickness $G_2=25$ [mm]				
4600-4650	2.228	2.820	0.592	2.048
4650-4700	2.041	2.724	0.682	2.507
4700-4750	1.678	2.547	0.868	3.624
4750-4800	1.848	2.311	0.463	1.943
For pads worn to thickness $G_3=35$ [mm]				
4600-4650	1.997	3.825	1.828	5.647
4650-4700	2.263	3.672	1.408	4.203
4700-4750	2.259	3.641	1.381	4.145
4750-4800	2.335	3.506	1.171	3.531

of the values of vibration accelerations on the right and left sides of the brake disc during braking for three cases of friction material thickness in the frequency function for the 4600-4700 Hz band.

Analyzing the results of vibration of the friction pads on both sides of the brake disc during braking, it is found that the analysis of lining vibration acceleration in the frequency domain relative to the analysis in the field of amplitude allows observation of a greater difference in the vibration of the right and left pad of the brake disc. The dynamics of changes is in the range of 4.6-7.2 dB for new pads, 2-3.6 dB for worn pads up to 25 mm thick and 3.5-5.6 dB for pads worn up to 15 mm thick. In the case of amplitude analysis, the differences in right and left vibration of the disc are in the range of 1-3 dB depending on the surface condition of the friction pads.

The paper [30] presents the results of vibroacoustic tests of a railway disc brake in which it was shown that the 4600-4700 Hz frequency band enables the assessment of the disc condition of a railway brake. In contrast, pulse tests of the main disc brake assemblies showed that the 4400-4600 Hz band is a common resonance band of such elements as the disc, friction pads and a complex lever mechanism.

Based on the vibroacoustic tests in the field of amplitudes and time, it was found that the non-uniformity of the vibrations of the right and left friction pad is the result of disturbances in the braking process. It was shown that this is caused by the uneven mass distribution of the elements of the lever system of the right and left side of the brake disc and friction in the pin joints of the mechanism. Consequently, the disc is not pressed by the pads with equal force, which would result from the design and assumptions of a symmetrical brake lever mechanism. In a broader sense, the demonstrated irregularity in the pressure of the brake pads on the disc may also affect the extension of the braking distance.

8. Conclusion

The article presents the results of the author's tests on a certified brake station for testing brakes of rail vehicles in the field of tribology, thermovision and vibroacoustics. Based on these tests, it was proved that the brakes of the right and left of the disc brake friction pair were uneven. It was found that the propagation of unfavorable vibrations and noise through the lever system may also result from the geometry of the braking system. The conducted research proves that the current models of vibration and noise in braking systems are insufficient

and take into account only the case of interaction of one friction element with the brake disc. Due to the design of the lever system, which should uniformly transfer the force from the brake cylinder to the friction pads, the friction phenomena and vibrations are different. It is caused by the uneven mass distribution of the elements of the right and left sides of the clamping mechanism, changes in the geometry of the system and friction in the kinematic nodes.

Uneven weight distribution of the braking system components relative to the right and left sides of the brake disc and friction in the bolt connections cause the following effects:

- an increase in vibration acceleration by an average of 25% on the cast from the brake cylinder side relative to the cast from the brake piston rod side in the entire braking process based on analysis in the field of amplitude of acceleration of friction lining vibrations,
- increase in vibration acceleration by approx. 50% on the cast from the brake cylinder side relative to the cast on the piston rod side in the 4600-4800 Hz frequency band by analyzing the vibration acceleration signals in the frequency domain,
- increased wear of the friction linings on the brake cylinder side by approx. 10-18% compared to the friction linings on the brake piston rod side,
- an increase in the average temperature of the friction linings by approx. 15-17% located on the side of the lighter brake cylinder relative to the heavier piston rod.

The paper shows that the unevenness in the mass distribution of the right and left side of the lever system is unfavorable from the point of the braking process. This results, differences in the value of forces acting on the disc. Vibrations on one side of the disc are intensified, which disturbs the braking process and may cause an increase in the braking distance.

Further work is planned to develop a model of a new lever mechanism, characterized by equal mass distribution of the right and left sides of the disc and a constant value of forces acting on the disc regardless of friction pad wear. Then, kinematic and dynamic analyses of the classic lever system (presented in the paper) in relation to the new one will be carried out, and an attempt will be made to carry out comparative tests on a brake stand.

References

1. Babishin V, Taghipour S. An algorithm for estimating the effect of maintenance on aggregated covariates with application to railway switch point machines. *Eksploatacja i Niezawodność - Maintenance and Reliability* 2019; 21(4): 619-630, <https://doi.org/10.17531/ein.2019.4.11>.
2. Bowden FP, Leben L. The nature of sliding and the analysis of friction. *Royal Society of London Proceedings Series A Mathematics Physics and Engineering Science* 1939; 169: 371-391, <https://doi.org/10.1098/rspa.1939.0004>.
3. Brooks PC, Crolla DA, Lang AM, Schafer DR. Eigenvalue sensitivity analysis applied to disc brake squeal. In: *Braking of Road Vehicles*. Bury St. Edmunds, England: Institution of Mechanical Engineers, Mechanical Engineering Publications Limited, 1993: 135-143.
4. Earles SWE, Chambers PW. Disc brake squeal noise generation: predicting its dependency on system parameters including damping. *International Journal of Vehicle Design* 1987; 8: 538-552.
5. European Standard EN 14535-3:2015. Railway applications - Brake discs for railway rolling stock - Part 3: Brake discs, performance of the disc and the friction couple, classification: 12-16.
6. European Standard EN 14535-1:2005. Railway applications - Brake discs for railway rolling stock - Part 1: Brake discs pressed or shrunk onto the axle or drive shaft, dimensions and quality requirements: 22-23.
7. Fosberry RAC, Holubecki A. Disc brake squeal: its mechanism and suppression. Technical Report. Motor Industry Research Association 1961; 1: 34-36.
8. Ghazaly NM, El-Sharkawy M, Ahmed I. A Review of Automotive Brake Squeal Mechanisms. *Journal of Mechanical Design and Vibration* 2013; 1(1): 5-9.
9. Gill A, Kadziński A. The determination procedure of the onset of the object wear-out period based on monitoring of the empirical failure intensity function. *Eksploatacja i Niezawodność - Maintenance and Reliability* 2015; 17(2): 282-287, <https://doi.org/10.17531/ein.2015.2.16>.
10. Glowacz A, Glowacz W, Kozik J, Piech K, Gutten M, Caesarendra W, Liu H, Brumercik F, Irfan M, Khan F. Detection of Deterioration of Three-phase Induction Motor using Vibration Signals. *Measurement Science Review* 2019; 19(6): 241-249, <https://doi.org/10.2478/msr-2019-0031>.
11. Glowacz A. Fault diagnosis of electric impact drills using thermal imaging. *Measurement* 2021; 171: 1-11, <https://doi.org/10.1016/j.measurement.2020.108815>.
12. Glowacz A. Acoustic fault analysis of three commutator motors. *Mechanical Systems and Signal Processing* 2019; 133: 1-17, <https://doi.org/10.1016/j.ymssp.2019.07.007>.
13. Hu Y, Wang S, Ai X. Research of the Vibration Source Tracking in Phase-Sensitive Optical Time-Domain Reflectometry Signals Based by Image Processing Method. *Algorithms* 2018; 11(8): 1-16, <https://doi.org/10.3390/a11080117>.
14. Jarvis RP, Mills B. Vibrations induced by friction. *Proceedings of the Institution of Mechanical Engineers* 1963; 178(32): 847-857, <https://doi.org/10.1177/0020348363178001124>.
15. Kinkaid NM, O'Reilly OM, Papadopoulos P. Automotive disc brake squeal. *Journal of Sound and Vibration* 2003; 267: 105-166, [https://doi.org/10.1016/S0022-460X\(02\)01573-0](https://doi.org/10.1016/S0022-460X(02)01573-0).
16. Konowrocki R, Chojnacki A. Analysis of rail vehicles' operational reliability in the aspect of safety against derailment based on various methods of determining the assessment criterion. *Eksploatacja i Niezawodność - Maintenance and Reliability* 2020; 22(1): 73-85, <https://doi.org/10.17531/ein.2020.1.9>.
17. Lang AM, Smales H. An approach to the solution of disc brake vibration problems. in: *Braking of Road Vehicles*. Automobile Division of the Institution of Mechanical Engineers. Suffolk: Mechanical Engineering Publications Limited 1993: 223-231.
18. Meierhofer A, Hardwick C, Lewis R, Six K, Dietmaier P. Third body layer-experimental results and a model describing its influence on the traction coefficient. *Wear* 2014; 314: 148-154, <https://doi.org/10.1016/j.wear.2013.11.040>.
19. Merkisz J, Rymaniak Ł. The assessment of vehicle exhaust emissions referred to CO₂ based on the investigations of city buses under actual conditions of operation. *Eksploatacja i Niezawodność - Maintenance and Reliability* 2017; 19(4): 522-529, <https://doi.org/10.17531/ein.2017.4.5>.
20. Millner N. An analysis of disc brake squeal. Technical Report 780332, SAE 1978: 22-24, <https://doi.org/10.4271/780332>.
21. Mills HR. Brake squeak. Technical Report 9000 B, Institution of Automobile Engineers 1938: 13-17.
22. Murakami H, Tsunada N, Kitamura T. A study concerned with a mechanism of disc-brake squeal. *SAE Transactions* 1984; 93(5): 604-616, <https://doi.org/10.4271/841233>.
23. North MR. Disc brake squeal, in: *Braking of Road Vehicles*. London: Automobile Division of the Institution of Mechanical Engineers, Mechanical Engineering Publications Limited 1976: 169-176.
24. Qu Y, Xie F, Su H, Meng G. Numerical analysis of stick-slip induced nonlinear vibration and acoustic responses of composite laminated plates with friction boundaries. *Composite Structures* 2021; 258: 1-12, <https://doi.org/10.1016/j.compstruct.2020.113316>.
25. Rudolph M, Popp K. The Influence of Contact Properties on Friction-Induced Brake Vibrations. *Proceedings of the 3rd Contact Mechanics International Symposium* 2001: 125-132, https://doi.org/10.1007/978-94-017-1154-8_14.
26. Rudolph M, Popp K. Brake squeal. In: Popp K. (Ed.), *Detection, Utilization and Avoidance of Nonlinear Dynamical Effects in Engineering Applications*. Final Report of a Joint Research Sponsored by the German Federal Ministry of Education and Research, Shaker, Aachen 2001: 197-225.
27. Saumweber E. Auslegung und Leistungsgrenzen von Scheibenbremsen. *ZEV-Glases Annalen* 1988; 112(4): 139-143.
28. Sawczuk W. Application of selected frequency characteristics of vibration signal for the evaluation of the braking process for railway disc brake. *Diagnostyka* 2015; 16(3): 33-38.
29. Sawczuk W. Application of vibroacoustic diagnostics to evaluation of wear of friction pads rail brake disc. *Eksploatacja i Niezawodność - Maintenance and Reliability* 2016; 18(4): 565-571, <https://doi.org/10.17531/ein.2016.4.11>.
30. Sawczuk W, Szymański GM. Diagnostics of the railway friction disc brake based on the analysis of the vibration signals in terms of resonant frequency. *Archive of Applied Mechanics* 2016; 86: 1-15.

31. Selech J, Andrzejczak K. An aggregate criterion for selecting a distribution for times to failure of components of rail vehicles. *Eksploracja i Niezawodność - Maintenance and Reliability*, 2020; 22(1): 102-111, <https://doi.org/10.17531/ein.2020.1.12>.
32. Shen X, Lu L, Zeng D. Fatigue failure analysis of high strength bolts used for high-speed railway vehicle braking discs. *Engineering Failure Analysis* 2020; 115: 1-16, <https://doi.org/10.1016/j.engfailanal.2020.104661>.
33. Shi LB, Wang F, Ma L, Liu QY, Guo J, Wang WJ. Study of the friction and vibration characteristics of the braking disc/pad interface under dry and wet conditions. *Tribology International* 2018; 127: 553-544, <https://doi.org/10.1016/j.triboint.2018.07.012>.
34. Sinclair D. Frictional vibrations. *Transactions of the American Society of Mechanical Engineers. Journal of Applied Mechanics* 1955; 77: 207-213.
35. Singh S, Kumar R. Evaluation of human error probability of disc brake unit assembly and wheel set maintenance of Railway Bogie. *Procedia Manufacturing* 2015; 3: 3041-3048, <https://doi.org/10.1016/j.promfg.2015.07.849>.
36. Sinou JJ, Thouverez F, Jezequel L. Analysis of friction and instability by the centre manifold theory for a non-linear sprag-slip model. *Journal of Sound and Vibration* 2003; 265: 527-559, [https://doi.org/10.1016/S0022-460X\(02\)01453-0](https://doi.org/10.1016/S0022-460X(02)01453-0).
37. Spurr RT. A theory of brake squeal. *Proceedings of the Automobile Division. Institution of Mechanical Engineers* 1961-1962; (1): 33-52, https://doi.org/10.1243/PIME_AUTO_1961_000_009_02.
38. Szymański GM, Tomaszewski F. Diagnostic of automatic compensators of valve clearance in combustion engine with the use of vibration signal. *Mechanical Systems and Signal Processing* 2016; 68-69: 479-490, <https://doi.org/10.1016/j.ymssp.2015.07.015>.
39. Świdorski A, Borucka A, Jacyna-Golda I, Szczepański E. Wear of brake system components in various operating conditions of vehicle in the transport company. *Eksploracja i Niezawodność - Maintenance and Reliability* 2019; 21(1): 1-9, <https://doi.org/10.17531/ein.2019.1.1>.
40. Tan Y, Zhang H, Zhou Y. A Simple-to-Implement Fault Diagnosis Method for Open Switch Fault in Wind System PMSG Drives without Threshold Setting. *Energies* 2018; 11(10): 1-18, <https://doi.org/10.3390/en1102571>.
41. Triches M, Gerges SNY, Jordan R. Analysis of brake squeal noise using finite element method. *Applied Acoustic* 2008; 69(2): 147-162, <https://doi.org/10.1016/j.apacoust.2007.10.003>.
42. UIC Code 541-3: Brakes - Disc brakes and their application - General conditions for the approval of brake pads. 7th edition, January 2010.
43. Wang XC, Huang B, Wang RL, Mo JL, Ouyang H. Friction-induced stick-slip vibration and its experimental validation. *Mechanical Systems and Signal Processing* 2020; 142: 2-21, <https://doi.org/10.1016/j.ymssp.2020.106705>.
44. Zhao X, Gräbner N, Wagner U. Avoiding creep groan: Investigation on active suppression of stick-slip limit cycle vibrations in an automotive disk brake via piezoceramic actuators. *Journal of Sound and Vibration* 2019; 441: 174-186, <https://doi.org/10.1016/j.jsv.2018.10.049>.